

Numerical homogenization for non-linear monotone elliptic problems

Barbara Verfürth[†]

Abstract. In this work we introduce and analyze a new multiscale method for non-linear monotone elliptic equations in the spirit of the Localized Orthogonal Decomposition. A problem-adapted multiscale space is constructed by solving linear local fine-scale problems which is then used in a generalized finite element method. The linearity of the fine-scale problems allows their localization and, moreover, makes the method very efficient to use. Both a Galerkin and a Petrov-Galerkin variant with only modified test functions are analyzed. The new method gives optimal a priori error estimates up to linearization errors beyond periodicity and scale separation and without assuming higher regularity of the solution. Several numerical examples including stationary Richards equation confirm the theory and underline the applicability of the method.

Key words. multiscale method; numerical homogenization; non-linear monotone elliptic problem; a priori error estimates

AMS subject classifications. 65N15, 65N30, 35J60, 74Q15

1. Introduction

Linear constitutive laws like Hooke's law in mechanics, Ohm's law in electromagnetics, or Darcy's law in fluid flow are very popular, but they are often not accurate enough in practical applications, for instance for high intensities. Instead, non-linear effects in the constitutive laws have to be taken into account which are often experimentally found and determined, see [40] for a general overview. In this article, we consider as model problem the following non-linear monotone elliptic equation

$$-\nabla \cdot (A(x, \nabla u)) = f,$$

where the exact assumptions as well as boundary conditions are specified later. It is a representative model problem for quasi-linear partial differential equations (PDEs) as they occur in mean curvature flow or for non-Newtonian fluids. Note that this class of problems is far more challenging than semi-linear PDEs, where the non-linearities do not appear in the highest derivative. The transition from linear to non-linear problems comes with huge additional challenges for the numerical treatment and analysis. As an illustrating example we mention optimal order L^2 -estimates for the finite element method: The classical Aubin-Nitsche trick for linear problems is not applicable, so that, for a long time, only optimal order estimates in the energy norm [10] were known, see [5] and the discussion therein. A similar observation applies to the effect of numerical integration, see [16].

With the view on practical applications such as fluid flow or elasticity, we do not only have to consider non-linear constitutive laws as discussed above, but also have to consider (spatial) multiscale features in the material coefficients (here, in A). For instance, a fluid such as groundwater

[†]Institut für Mathematik, Universität Augsburg, Universitätsstr. 14, D-86159 Augsburg

flows over large distances, while the properties of the soil changes over small distances and thereby influences the overall groundwater flow, see, e.g., [38]. Hence, for applications such as the (quasi-linear) porous medium equation, A is subject to rapid variations and/or discontinuities on fine spatial scales or even a cascade of (non-separable) scales. This coincidence of multiscale features and non-linear material laws makes the problem intractable for standard (problem-independent) methods. For example, the standard finite element method [2, 10, 16] will only give optimal convergence in the asymptotic regime, i.e., if the mesh resolves all features and scales present in the coefficient, which is prohibitively expensive even with today's computational resources.

In the case of spatially periodic A (with period $\varepsilon \ll 1$), homogenization results using two-scale convergence [7, 30] prove that the solutions of the above model problem converge to the solution of an again monotone elliptic (homogenized) problem for $\varepsilon \rightarrow 0$. The non-linear effective diffusion tensor can be computed by solving non-linear so-called cell problems. The (finite element) heterogeneous multiscale method is inspired by this analytical process and it is studied successfully for non-linear problems in a series of papers [1, 3, 4, 6, 20, 24]. In most cases, the macroscopic non-linear form involves non-linear reconstruction operators which require the solution of non-linear cell problems at each macroscopic quadrature point and thereby incorporate the necessary fine-scale information. For parabolic equations, [4] linearizes the macroscopic and cell computations using information from the previous time step. The sparse multiscale FEM [26] is also motivated by homogenization results and tries to reduce the complexity of solving cell problems and a homogenized equation by the introduction of sparse approximations. Another idea to cope with multiscale problems is to modify or enrich the standard finite element basis by problem-adapted functions. This idea is used for instance in the (generalized) multiscale finite element method, for which non-linear problems are discussed in [9, 12, 13]. Again non-linear problems have to be solved locally to construct the problem-adapted functions.

The main contribution of this article is the introduction of a new multiscale method for non-linear monotone elliptic problems and its numerical analysis. The idea is to construct a multiscale (test) space by solving local fine-scale problems in the spirit of the Localized Orthogonal Decomposition (LOD) [31, 34]. In contrast to the above discussed methods, the basis construction only requires the solution of *linear* problems and hence is embarrassingly easy to implement and use. Moreover, this linearization idea drastically reduces the computational effort for generating a problem-dependent (multiscale) basis and thereby provides a conceptually new view on the treatment of non-linear multiscale problems. We derive optimal convergence rates (with respect to the mesh size H) up to linearization errors without any assumption on the regularity of the exact solution or special properties such as periodicity or scale separation for the coefficient. Possible techniques to estimate the occurring linearization errors are also discussed. Extensive numerical experiments show the good performance of the method in agreement with the theoretical estimates. We study periodic as well as completely random multiscale coefficients and also include models for stationary Richards equation, for instance with a high contrast channel. Because of the relation between the LOD and homogenization theory for periodic coefficients on suitable meshes [17], our numerical experiments with locally periodic diffusion tensors indicate that the presented idea of linearizing the fine-scale problems might be transferable to the Heterogeneous Multiscale Method in [20, 27]. Besides several linear problem classes, the LOD has already been studied for semi-linear equations [22] and a non-linear eigenvalue problem related to the Gross-Pitaevskii equation [23]. These problems, however, are only semi-linear and can therefore be handled easier. Yet, we emphasize that these previous works can be re-interpreted in the current framework. We mention the close connections of the LOD to (analytical) homogenization [17, 36], domain decomposition iterative solvers [28, 29, 36], and so-called gamblets [32, 33]. Hence, the current approach can give interesting and useful insights in these areas for non-linear problems as well, a direction that is not pursued further in this work.

The article is organized as follows: Section 2 introduces the setting and the standard finite ele-

ment discretization. We introduce the multiscale method including linearization and localization in Section 3. The arising errors are analyzed in Section 4. Finally, we present several numerical experiments confirming our theory and showing possible applications in Section 5.

2. Problem formulation and discretization

In this section we formulate the considered model problem and introduce necessary finite element prerequisites. We use standard notation on Sobolev spaces. Throughout the whole article, let $\Omega \subset \mathbb{R}^d$ be a bounded Lipschitz domain. For a subdomain $D \subset \Omega$, let $\|\cdot\|_{0,D}$, $\|\cdot\|_{1,D}$, and $|\cdot|_{1,D}$ denote the standard $L^2(D)$ -norm, $H^1(D)$ -norm, and $H^1(D)$ -semi norm, respectively. Furthermore, $(\cdot, \cdot)_D$ denotes the standard L^2 scalar product on D . We will omit the subscript D if it equals the full computational domain Ω .

2.1. Model problem

We consider the following non-linear elliptic problem: Find $u : \Omega \rightarrow \mathbb{R}$ such that

$$\begin{aligned} -\nabla \cdot (A(x, \nabla u)) &= f \quad \text{in } \Omega, \\ u &= 0 \quad \text{on } \partial\Omega \end{aligned} \tag{2.1}$$

with a right-hand side $f \in L^2(\Omega)$. The corresponding weak formulation, with which we will work in the following, reads: Find $u \in H_0^1(\Omega)$ such that

$$\mathcal{B}(u; v) := (A(x, \nabla u), \nabla v)_\Omega = (f, v)_\Omega \quad \text{for all } v \in H_0^1(D). \tag{2.2}$$

For simplicity, we restrict ourselves to homogeneous Dirichlet boundary conditions, but non-homogeneous and Neumann boundary conditions could be treated as well, see [21]. Moreover, we focus on non-linearities in the highest derivative only, additional (non-linear) low-order terms can easily be handled as well, cf. [22]. We now specify the assumptions on A , which guarantee existence and uniqueness of a solution.

Assumption 2.1. *The non-linearity $A : \Omega \times \mathbb{R}^d \rightarrow \mathbb{R}^d$ satisfies*

1. $A(\cdot, \xi) \in L^\infty(\Omega; \mathbb{R}^d)$ for all $\xi \in \mathbb{R}^d$ and $A(x, \cdot) \in C^1(\mathbb{R}^d; \mathbb{R}^d)$ for almost every $x \in \Omega$;
2. there is $\Lambda > 0$ such that $|A(x, \xi_1) - A(x, \xi_2)| \leq \Lambda |\xi_1 - \xi_2|$ for almost every $x \in \Omega$ and all $\xi_1, \xi_2 \in \mathbb{R}^d$;
3. there is $\lambda > 0$ such that $(A(x, \xi_1) - A(x, \xi_2)) \cdot (\xi_1 - \xi_2) \geq \lambda |\xi_1 - \xi_2|^2$ for almost every $x \in \Omega$ and all $\xi_1, \xi_2 \in \mathbb{R}^d$;
4. $A(x, 0) = 0$ for almost every $x \in \Omega$.

Assumption 2.1 implies that

$$|\mathcal{B}(v_1; \psi) - \mathcal{B}(v_2; \psi)| \leq \Lambda |v_1 - v_2|_1 |\psi|_1 \quad \text{and} \quad \mathcal{B}(v; v - \psi) - \mathcal{B}(\psi; v - \psi) \geq \lambda |v - \psi|_1^2$$

for all $v, v_1, v_2, \psi \in H_0^1(\Omega)$. Therefore, the model problem (2.2) has a unique solution $u \in H_0^1(\Omega)$, which satisfies

$$|u|_1 \leq \Lambda/\lambda \|f\|_0, \tag{2.3}$$

see [10, Chapter 5]. As discussed in the introduction, we implicitly assume that A is subject to rapid oscillations or discontinuities on a rather fine scale with respect to the spatial variable x .

We write $a \lesssim b$ in short for $a \leq Cb$ with a constant C independent of the mesh size H and the oversampling parameter m introduced later. However, C may depend on the monotonicity and Lipschitz constants λ, Λ of A (cf. Assumption 2.1).

2.2. Finite element discretizations

We cover Ω with a regular mesh \mathcal{T}_H consisting of simplices; however, a mesh with quadrilaterals would equally be possible. The mesh is assumed to be shape regular in the sense that the aspect ratio of the elements of \mathcal{T}_H is bounded uniformly from below. We introduce the mesh size $H = \max_{T \in \mathcal{T}_H} \text{diam } T$ and assume that this is rather coarse, in particular, \mathcal{T}_H does not resolve the possible heterogeneities in A . We discretize the space $H_0^1(\Omega)$ with the lowest order Lagrange elements over \mathcal{T}_H , and denote this space by V_H . This means that $V_H = H_0^1(\Omega) \cap \mathcal{S}^1(\mathcal{T}_H)$, where $\mathcal{S}^1(\mathcal{T}_H)$ denotes the space of element-wise polynomials of total degree ≤ 1 .

The standard finite element method now seeks a (discrete) solution $u_H \in V_H$ such that

$$\mathcal{B}(u_H; v_H) = (f, v_H)_\Omega \quad \text{for all } v_H \in V_H.$$

This results in a non-linear system which can be (approximatively) solved with Newton's method. If we neglect numerical errors introduced by the inexact solving in Newton's method, it is well-known that the properties of A and Galerkin orthogonality imply

$$|u - u_H|_1 \lesssim \inf_{v_H \in V_H} |u - v_H|_1, \quad (2.4)$$

see [10, Chapter 5]. This quasi-optimality by the way holds for any conforming subset $\tilde{V}_H \subset H_0^1(\Omega)$. For the standard finite element method it is furthermore well-known to have the following (a priori) error estimates with $k > 0$

$$\|u - u_H\|_1 \leq CH^k \|u\|_{H^{1+k}(\Omega)} \quad \text{and} \quad \|u - u_H\|_0 \leq CH^{k+1} \|u\|_{H^{1+k}(\Omega)},$$

see [2]. In the above error estimates higher regularity (more than $H_0^1(\Omega)$) of the exact solution is required. However, the regularity of u may be very low for non-linearities A with spatial discontinuities. Even if the exact solution u satisfies sufficient higher regularity, the corresponding norms $\|u\|_{H^{k+1}(\Omega)}$ depend on spatial derivatives of A which behave like ε^{-q} for some $q \geq 1$ for coefficients varying on a scale ε . In practice this implies that H needs to be at least ε in order to observe the linear convergence in the H^1 -norm. In other words, for small ε , there is a large pre-asymptotic region where no error estimates are available and the error stagnates (at a high level) in practice.

The goal of the multiscale method presented in Section 3 is to circumvent both issues (higher regularity of the solution and dependence on the variations of A). At the heart of the method is the choice of a suitable interpolation operator and we now introduce the required properties as well as an appropriate example. Let $I_H : H_0^1(\Omega) \rightarrow V_H$ denote a bounded local linear projection operator, i.e., $I_H \circ I_H = I_H$, with the following stability and approximation properties for all $v \in H_0^1(\Omega)$

$$|I_H v|_{1,T} \lesssim |v|_{1,N(T)}, \quad (2.5)$$

$$\|v - I_H v\|_{0,T} \lesssim H |v|_{1,N(T)}. \quad (2.6)$$

where the constants are independent of H and $N(T) := \{K \in \mathcal{T}_H : K \cap T \neq \emptyset\}$ denotes the neighborhood of an element. A possible choice (which we use in our implementation of the method) is to define $I_H := E_H \circ \Pi_H$. On each element $T \in \mathcal{T}_H$, the affine function $(\Pi_H v)|_T$ is the best approximation of $v \in H_0^1(\Omega)$ in the $\|\cdot\|_{0,T}$ -norm, and E_H is the averaging operator that maps discontinuous functions in $\mathcal{S}^1(\mathcal{T}_H)$ to V_H by assigning to each free vertex the arithmetic mean of the corresponding function values of the neighboring cells, that is, for any $v \in \mathcal{S}^1(\mathcal{T}_H)$ and any vertex z of \mathcal{T}_H ,

$$(E_H(v))(z) = \sum_{T \in \mathcal{T}_H, z \in T} v|_T(z) / \text{card}\{K \in \mathcal{T}_H, z \in K\}.$$

For further details on suitable interpolation operators we refer to [15].

3. Computational multiscale method

In the following, we assume that an interpolation operator $I_H : H_0^1(\Omega) \rightarrow V_H$ satisfying the projection property as well as (2.6) and (2.5) is at hand. Abbreviating $W := \ker I_H$, we have the splitting $H_0^1(\Omega) = V_H \oplus W$. The main idea of the Localized Orthogonal Decomposition [31, 34] is to make this splitting problem-dependent. For instance, in the linear elliptic case the splitting is orthogonalized with respect to the energy scalar product. Below, we discuss how this idea can be transferred to the non-linear case, which turns out to be highly non-trivial. We introduce a linearization procedure in the next subsection which makes the computation of a multiscale space in the spirit of the LOD possible. Afterwards, we present the localized computation of the new multiscale basis functions.

3.1. An ideal method and its linearization

Motivated by linear elliptic equations, one could (naively) try to introduce a Galerkin method over a subset $V_H^{\text{nl,ms}} \subset H_0^1(\Omega)$, i.e., we seek $u_H^{\text{nl,ms}}$ such that

$$\mathcal{B}(u_H^{\text{nl,ms}}; v) = (f, v)_\Omega \quad \text{for all } v \in V_H^{\text{nl,ms}},$$

where the set $V_H^{\text{nl,ms}}$ is defined via

$$\mathcal{B}(v_H^{\text{nl,ms}}; w) = 0 \quad \text{for all } v_H^{\text{nl,ms}} \in V_H^{\text{nl,ms}} \quad \text{and all } w \in W. \quad (3.1)$$

This is the orthogonalization idea behind the original method, see [31, 34]. Due to the quasi-optimality (2.4) and the properties (2.5) and (2.6) of I_H , one obtains the a priori error estimate

$$\|u - u_H^{\text{nl,ms}}\|_1 \lesssim H \|f\|_0$$

with optimal rate in the mesh size, independent of the regularity of the continuous solution u . This estimate is derived similar to the linear case and we refer to [31, 34] for details. Because of the non-linearity of \mathcal{B} in its first argument, however, $V_H^{\text{nl,ms}}$ is no longer a linear subspace. To be more precise, we consider the usual construction of $V_H^{\text{nl,ms}}$: It holds $V_H^{\text{nl,ms}} = (\text{id} - \mathcal{Q}^{\text{nl}})V_H$, where $\mathcal{Q}^{\text{nl}} : V_H \rightarrow W$ solves

$$\mathcal{B}(v_H - \mathcal{Q}^{\text{nl}}v_H; w) = 0 \quad \text{for all } w \in W. \quad (3.2)$$

Here, we clearly see that \mathcal{Q}^{nl} is a non-linear operator. Therefore, it is by no means clear whether the proposed multiscale method is at all well defined. Even if this is the case, the method is very complicated as it involves two coupled non-linear problems, where the one for the generation of the correction is additionally posed on the fine scale. Hence, we need to simplify in particular the generation of the problem-adapted multiscale basis.

Here, we propose the following simple yet effective linearization approach. We define the *linear* correction operator $\mathcal{Q} : V_H \rightarrow W$ via

$$\mathcal{A}(v_H - \mathcal{Q}v_H, w) = 0 \quad \text{for all } w \in W, \quad (3.3)$$

where the bilinear form \mathcal{A} is defined as

$$\mathcal{A}(v, \psi) := (\mathfrak{A}(x)\nabla v, \nabla \psi)_\Omega, \quad \text{with } \mathfrak{A} := D_\xi A(\cdot, 0) \in L^\infty(\Omega; \mathbb{R}^{d \times d}).$$

Due to Assumption 2.1, \mathfrak{A} is uniformly elliptic and bounded, i.e.,

$$\mathfrak{A}\xi \cdot \xi \geq \lambda|\xi|^2 \quad \text{and} \quad |\mathfrak{A}\xi| \leq \Lambda|\xi| \quad \text{for all } \xi \in \mathbb{R}^d, \quad (3.4)$$

see [27, Lemma 6.5.2]. Hence, the linear corrector problem (3.3) has a unique solution. Moreover, it is the linearization of the non-linear problem (3.2) around zero. Alternatively, (3.3) can be interpreted as one step of Newton's method applied to (3.1) with initial guess zero.

For simplicity of exposition we make the following assumption.

Assumption 3.1. \mathfrak{A} is symmetric.

We could also continue with a non-symmetric diffusion tensor in (3.3), but then we also need the adjoint of \mathcal{Q} , which would clutter notation in the following.

Having linearized the computation of the correction operator, we define the linear multiscale space $V_H^{\text{ms}} := (\text{id} - \mathcal{Q})V_H$. This problem-adapted space is used in a Galerkin method to seek $u_H^{\text{ms}} \in V_H^{\text{ms}}$ such that

$$\mathcal{B}(u_H^{\text{ms}}; v_H^{\text{ms}}) = (f, v_H^{\text{ms}})_\Omega \quad \text{for all } v_H^{\text{ms}} \in V_H^{\text{ms}}. \quad (3.5)$$

Let $\{\lambda_z\}_z$ be the nodal basis of V_H (i.e., the standard functions). Then $\{\lambda_z - \mathcal{Q}\lambda_z\}_z$ forms a basis of V_H^{ms} . Note that this requires only to solve linear problems. After this basis has been (pre-)computed, the non-linear problem (3.5) can be solved with Newton's method, which is rather cheap since the dimension of the multiscale space is small (note $\dim(V_H^{\text{ms}}) = \dim(V_H)$). In general, linear problems are much easier and cheaper to solve than non-linear problems (of the same dimension), which is the appealing advantage of (3.3) in comparison to (3.2) – apart from the discussed well-posedness issues.

3.2. Localization of the basis generation

As in the linear case, the corrector problems (3.3) are global fine-scale problems, which are as expensive to solve as the solution of a (linear) multiscale model problem on a fine-scale mesh resolving the oscillations and discontinuities of A . However, due to the spectral bounds (3.4), we can localize these corrector problems in the well-known way for the linear case. To this end, we define the neighborhood

$$N(T) = \bigcup_{K \in \mathcal{T}_H, T \cap K \neq \emptyset} K$$

associated with an element $T \in \mathcal{T}_H$. Thereby, for any $m \in \mathbb{N}_0$, the m -layer patches are defined inductively via $N^{m+1}(T) = N(N^m(T))$ with $N^0(T) := T$. The shape regularity implies that there is a bound $C_{\text{ol},m}$ (depending only on m) of the number of the elements in the m -layer patch, i.e.,

$$\max_{T \in \mathcal{T}_H} \text{card}\{K \in \mathcal{T}_H : K \subset N^m(T)\} \leq C_{\text{ol},m}. \quad (3.6)$$

Throughout this article, we assume that \mathcal{T}_H is quasi-uniform, which implies that $C_{\text{ol},m}$ grows at most polynomially with m .

We then define the truncated correction operator $\mathcal{Q}_m : V_H \rightarrow W$ as $\mathcal{Q}_m = \sum_{T \in \mathcal{T}_H} \mathcal{Q}_{T,m}$, where for any $v_H \in V_H$ the truncated element corrector $\mathcal{Q}_{T,m}v_H \in W(N^m(T)) := \{w \in W : w = 0 \text{ in } \Omega \setminus N^m(T)\}$ solves

$$\mathcal{A}_{N^m(T)}(\mathcal{Q}_{T,m}v_H, w) = \mathcal{A}_T(v_H, w) \quad \text{for all } w \in W(N^m(T)). \quad (3.7)$$

Here, \mathcal{A}_D denotes the restriction of the bilinear form \mathcal{A} to the subdomain $D \subset \Omega$. With the localized correction operator \mathcal{Q}_m , we set up the multiscale space $V_{H,m} := (\text{id} - \mathcal{Q}_m)V_H$. For each element $T \in \mathcal{T}_H$, we only have to solve d problems of type (3.7) with $v_H|_T = x_j$, $j = 1, \dots, d$, or precisely, the following cell problems: Find $q_{T,m}^{(j)} \in W(N^m(T))$, $j = 1, \dots, d$, such that

$$\int_{N^m(T)} \mathfrak{A} \nabla q_{T,m}^{(j)} \cdot \nabla w \, dx = \int_T \mathfrak{A} e_j \cdot \nabla w \, dx \quad \text{for all } w \in W(N^m(T)),$$

where e_j denotes the j th canonical unit vector. Denoting by $\{\lambda_z\}_z$ the standard hat functions, a basis of $V_{H,m}$ is hence given by

$$\left\{ \lambda_z - \sum_{T \in \mathcal{T}_H, z \in T} \sum_{j=1}^d \left(\frac{\partial}{\partial x_j} \lambda_z|_T \right) q_{T,m}^{(j)} \right\}_z.$$

The localized multiscale method consists of replacing V_H^{ms} by $V_{H,m}$ in (3.5). More precisely, we seek (in a Galerkin method) $u_{H,m} \in V_{H,m}$ such that

$$\mathcal{B}(u_{H,m}; v_{H,m}) = (f, v_{H,m})_\Omega \quad \text{for all } v_{H,m} \in V_{H,m}. \quad (3.8)$$

As mentioned before, problem (3.8) is solved with Newton's method, where the multiscale basis can be pre-computed. This requires the storage of all correctors, which can be very memory consuming since $q_{T,m}^{(j)}$ includes fine-scale features. If memory is a limiting factor, the correctors should better be computed on the fly inside each Newton iteration (less memory consuming, but potentially slightly slower). To avoid communication between the correctors, we introduce the Petrov-Galerkin method to seek $u_{H,m}^{PG} \in V_H$ such that

$$\mathcal{B}(u_{H,m}^{PG}; v_{H,m}) = (f, v_{H,m})_\Omega \quad \text{for all } v_{H,m} \in V_{H,m}. \quad (3.9)$$

In the Petrov-Galerkin method, $q_{T,j}$ and $q_{T',j}$ for $T, T' \in \mathcal{T}_H$ with $T \neq T'$ are never needed at the same time. Hence, these correctors can immediately be discarded once the contributions of element T to the linear system (which is set up in each Newton iteration) are assembled. Hence, when memory becomes the limiting factor, the Petrov-Galerkin variant is highly preferable in comparison to the Galerkin variant, see [14, 15], and we also use it in our numerical experiments. Note, however, that $u_{H,m}^{PG}$ in (3.9) only contains information on the coarse scale H . If one is interested in fine-scale information as well, one can easily post-process the Petrov-Galerkin solution $u_{H,m}^{PG}$ by introducing $u_{H,m}^{\text{LOD},PG} := (\text{id} - \mathcal{Q})u_{H,m}^{PG}$, a process frequently called upscaling. We emphasize that $u_{H,m}^{\text{LOD},PG}$ and $u_{H,m}$ lie in the same space $V_{H,m}$, but do not coincide in general.

Finally, we briefly mention that the present method is still semi-discrete since the corrector problems (3.7) are infinite-dimensional. The discretization procedure for them is equivalent to the case of linear elliptic equations: We introduce a second (fine) simplicial mesh \mathcal{T}_h of Ω which resolves all features of A . Denoting by $V_h = H_0^1(\Omega) \cap \mathcal{S}^1(\mathcal{T}_h)$ the corresponding lowest order Lagrange finite element space, we set $W_h(\mathbb{N}^m(T)) := \{w_h \in V_h : w_h = 0 \text{ in } \Omega \setminus \mathbb{N}^m(T), I_H w_h = 0\}$ and discretize (3.7) by solving over the space $W_h(\mathbb{N}^m(T))$ instead of $W(\mathbb{N}^m(T))$. In the following, we work with the semi-discrete version and emphasize that similar error estimates (with respect to a reference solution $u_h \in V_h$) can be shown in the fully discrete variant, as illustrated for the linear case, see [21, 25, 31].

4. Error analysis

Since the linearized corrector problem (3.3) is a standard elliptic problem, we have the following result on the localization error.

Proposition 4.1. *Assume that Assumptions 3.1 and 2.1 are fulfilled. Let \mathcal{Q} be the ideal linearized correction operator defined in (3.3) and \mathcal{Q}_m its truncated/localized version as defined via (3.7). There exists $0 < \beta < 1$ such that for any $v_H \in V_H$*

$$|(\mathcal{Q} - \mathcal{Q}_m)v_H|_1 \lesssim C_{\text{ol},m}^{1/2} \beta^m |v_H|_1.$$

Due to the spectral bounds (3.4) for \mathfrak{A} , Proposition 4.1 follows from the standard linear elliptic case in [21, 31, 34]. The main idea is that \mathcal{Q}_T decays exponentially fast (measured in m) away from T so that the localization error is small. With a slightly different localization strategy, the procedure can also be interpreted in the spirit of an iterative domain decomposition solver, see [28, 29].

We first discuss estimates for the Galerkin method (3.8) in Section 4.1 and then for the Petrov-Galerkin method (3.9) in Section 4.2. In both cases, (additional) error terms arise from the linearization, which we discuss separately in Section 4.3.

4.1. Error analysis for the Galerkin method

Since $V_{H,m}$ is a linear subspace of $H_0^1(\Omega)$, the Galerkin method (3.5) is automatically well defined, i.e., there exists a unique solution $u_{H,m}$. Its error to the exact solution in the H^1 -semi norm can be estimated as follows.

Theorem 4.2. *Let Assumptions 3.1 and 2.1 be fulfilled. Let u be the solution to (2.2) and $u_{H,m}$ the solution to (3.8). Then it holds that*

$$|u - u_{H,m}|_{1,\Omega} \lesssim (H + C_{\text{ol},m}^{1/2} \beta^m) \|f\|_{0,\Omega} + \eta_{\text{lin}}(u) \quad (4.1)$$

with the linearization error

$$\eta_{\text{lin}}(u) := \sup_{w \in W, |w|_1=1} |(A(x, \nabla(\text{id} - \mathcal{Q})I_H u), \nabla w)_\Omega|.$$

Proof. Since (3.8) defines a Galerkin method, the quasi-optimality (2.4) leads to

$$|u - u_{H,m}|_1 \lesssim \inf_{v_{H,m} \in V_{H,m}} |u - v_{H,m}|_1.$$

We choose $v_{H,m} = (\text{id} - \mathcal{Q}_m)I_H u = (\text{id} - \mathcal{Q})I_H u + (\mathcal{Q}_m - \mathcal{Q})I_H u$ and observe that the second term can directly be estimated using Proposition 4.1, the stability of I_H and (2.3).

Note that by definition $u - (\text{id} - \mathcal{Q})I_H u \in W$. Moreover, the stability of \mathcal{Q} , (2.5), and (2.3) imply $|u - (\text{id} - \mathcal{Q})I_H u|_1 \lesssim \|f\|_0$. Hence we obtain with the strong monotonicity of A (cf. Assumption 2.1) and the approximation property (2.6) that

$$\begin{aligned} & |u - (\text{id} - \mathcal{Q})I_H u|_1^2 \\ & \lesssim \int_\Omega [A(x, \nabla u) - A(x, \nabla(\text{id} - \mathcal{Q})I_H u)] \cdot \nabla(u - (\text{id} - \mathcal{Q})I_H u) \, dx \\ & = (f, u - (\text{id} - \mathcal{Q})I_H u)_\Omega - \int_\Omega A(x, \nabla(\text{id} - \mathcal{Q})I_H u) \cdot \nabla(u - (\text{id} - \mathcal{Q})I_H u) \, dx \\ & \lesssim (H \|f\|_0 + \eta_{\text{lin}}(u)) |u - (\text{id} - \mathcal{Q})I_H u|_1. \end{aligned}$$

Combination of this estimate with Proposition 4.1 as described above finishes the proof. \square

Up to the linearization error $\eta_{\text{lin}}(u)$, which is discussed in Section 4.3, the previous theorem is identical to the linear elliptic case [31]. In particular, if we choose $m \approx |\log(H)|$, we have linear convergence of the approximate solution to the exact one without any assumptions on the regularity of u or the variations of A . By Friedrich's inequality, the same estimate also holds for the L^2 -norm. In contrast to the linear case, the Aubin-Nitsche trick cannot be applied so that higher order convergence for non-linear problems is rather difficult to achieve, see the discussion in [2]. Using the idea of the elliptic projection in [2], we obtain an L^2 -estimate in Theorem A.1

in the Appendix. Roughly speaking, it yields quadratic convergence (up to (new) linearization errors) for the choice $m \approx |\log(H)|$.

By the stability of I_H we deduce an estimate for the error to $I_H u_{H,m}$, which describes the finite element part of the Galerkin solution.

Corollary 4.3. *Let Assumptions 3.1 and 2.1 be fulfilled. Let u be the solution to (2.2) and $u_{H,m}$ the solution to (3.8). Then it holds that*

$$\|u - I_H u_{H,m}\|_0 \lesssim H \inf_{v_H \in V_H} |u - v_H|_1 + \|u - u_{H,m}\|_0 + H|u - u_{H,m}|_1. \quad (4.2)$$

Proof. With the triangle inequality we split

$$\|u - I_H u_{H,m}\|_0 \leq \|u - I_H u\|_0 + \|I_H(u - u_{H,m})\|_0,$$

which finishes the proof together with the properties (stability, approximation, and projection) of I_H . \square

Note that the two last terms in (4.2) can be estimated via Theorem 4.2. For the L^2 -norm we also have the estimates from Theorem A.1 in the appendix. For $m \approx |\log(H)|$, these terms are at least of order H (up to linearization errors) and may even be of order H^2 (cf. the discussion in the appendix). Hence, the error $\|u - I_H u_{H,m}\|_0$ is at least of order H and might be up to order H^2 if u is sufficiently regular. If we assume L^2 -stability of I_H , i.e., $\|I_H v\|_0 \lesssim \|v\|_0$ for all $v \in H_0^1(\Omega)$, the estimate in Corollary 4.3 simplifies to

$$\|u - I_H u_{H,m}\|_0 \lesssim \inf_{v_H \in V_H} \|u - v_H\|_0 + \|u - u_{H,m}\|_0.$$

Together with Theorem A.1 this implies that the error in the finite element part of $u_{H,m}$ is dominated by the L^2 -best-approximation error in the finite element space.

4.2. Error analysis for the Petrov-Galerkin method

In contrast to the Galerkin method, it is a priori not clear whether a solution to (3.9) exists. In [37], an abstract theory concerning Petrov-Galerkin methods for non-linear problems is presented. It provides the existence of a unique discrete solution for sufficiently fine mesh size H as well as quasi-optimality if $D_\xi A$ is Lipschitz in its second argument in a neighborhood of ∇u (cf. the global Assumption 4.6) and the bilinear form $(D_\xi A(x, \nabla u) \nabla \cdot, \nabla \cdot)$ satisfies an inf-sup-condition over $V_H \times V_{H,m}$. The latter condition is examined in the next lemma.

Lemma 4.4. *Let u be the solution to (2.2) and let Assumptions 2.1 and 3.1 be satisfied. Then it holds*

$$\inf_{v_H \in V_H} \sup_{\psi_{H,m} \in V_{H,m}} \frac{|(D_\xi A(x, \nabla u) \nabla v_H, \nabla \psi_{H,m})|}{|v_H|_1 |\psi_{H,m}|_1} \gtrsim \frac{1 - \|D_\xi A(x, \nabla u) - \mathfrak{A}\|_{L^\infty} - C_{\text{ol},m}^{1/2} \beta^m}{1 + C_{\text{ol},m}^{1/2} \beta^m}. \quad (4.3)$$

Proof. We obtain by the definition of $V_{H,m}$ and upper and lower triangle inequalities that

$$\begin{aligned} & \inf_{v_H \in V_H} \sup_{\psi_{H,m} \in V_{H,m}} \frac{|(D_\xi A(x, \nabla u) \nabla v_H, \nabla \psi_{H,m})|}{|v_H|_1 |\psi_{H,m}|_1} \\ &= \inf_{v_H \in V_H} \sup_{\psi_H \in V_H} \frac{|(D_\xi A(x, \nabla u) \nabla v_H, \nabla (\text{id} - \mathcal{Q}_m) \psi_H)|}{|v_H|_1 |(\text{id} - \mathcal{Q}_m) \psi_H|_1} \end{aligned}$$

$$\begin{aligned}
&\geq \inf_{v_H \in V_H} \sup_{\psi_H \in V_H} \frac{|(D_\xi A(x, \nabla u) \nabla v_H, \nabla(\text{id} - \mathcal{Q})\psi_H)| - |(D_\xi A(x, \nabla u) \nabla v_H, \nabla(\mathcal{Q}_m - \mathcal{Q})\psi_H)|}{|v_H|_1 (|(\text{id} - \mathcal{Q})\psi_H|_1 + |(\mathcal{Q} - \mathcal{Q}_m)\psi_H|_1)} \\
&\geq \inf_{v_H \in V_H} \sup_{\psi_H \in V_H} \frac{|(D_\xi A(x, \nabla u) \nabla v_H, \nabla(\text{id} - \mathcal{Q})\psi_H)| - C_{\text{ol},m}^{1/2} \beta^m |v_H|_1 |(\text{id} - \mathcal{Q}_{T,m})\psi_H|_1}{(1 + C_{\text{ol},m}^{1/2} \beta^m) |v_H|_1 |(\text{id} - \mathcal{Q})\psi_H|_1},
\end{aligned}$$

where we used Proposition 4.1 and the norm equivalence

$$|\psi_H|_1 = |I_H(\text{id} - \mathcal{Q})\psi_H|_1 \lesssim |(\text{id} - \mathcal{Q})\psi_H|_1 \lesssim |\psi_H|_1$$

in the last step. We now need to replace $D_\xi A(x, \nabla u)$ by \mathfrak{A} to exploit the orthogonality of W and V_H^{ms} . This yields together with the ellipticity of \mathfrak{A}

$$\begin{aligned}
&\inf_{v_H \in V_H} \sup_{\psi_{H,m} \in V_{H,m}} \frac{|(D_\xi A(x, \nabla u) \nabla v_H, \nabla \psi_{H,m})|}{|v_H|_1 |\psi_{H,m}|_1} \\
&\gtrsim \inf_{v_H \in V_H} \sup_{\psi_H \in V_H} \frac{|\mathcal{A}(v_H, (\text{id} - \mathcal{Q})v_H)| - (\|\mathfrak{A} - D_\xi A(x, \nabla u)\|_{L^\infty} - C_{\text{ol},m}^{1/2} \beta^m) |(\text{id} - \mathcal{Q})\psi_H|_1 |v_H|_1}{(1 + C_{\text{ol},m}^{1/2} \beta^m) |v_H|_1 |(\text{id} - \mathcal{Q})\psi_H|_1} \\
&= \inf_{v_H \in V_H} \sup_{\psi_H \in V_H} \left[\frac{|\mathcal{A}((\text{id} - \mathcal{Q})v_H, (\text{id} - \mathcal{Q})v_H)|}{(1 + C_{\text{ol},m}^{1/2} \beta^m) |v_H|_1 |(\text{id} - \mathcal{Q})\psi_H|_1} \right. \\
&\quad \left. - \frac{(\|\mathfrak{A} - D_\xi A(x, \nabla u)\|_{L^\infty} - C_{\text{ol},m}^{1/2} \beta^m) |(\text{id} - \mathcal{Q})\psi_H|_1 |v_H|_1}{(1 + C_{\text{ol},m}^{1/2} \beta^m) |v_H|_1 |(\text{id} - \mathcal{Q})\psi_H|_1} \right] \\
&\gtrsim \frac{1 - \|D_\xi A(x, \nabla u) - \mathfrak{A}\|_{L^\infty} - C_{\text{ol},m}^{1/2} \beta^m}{1 + C_{\text{ol},m}^{1/2} \beta^m},
\end{aligned}$$

which finishes the proof. \square

If the linearization error $\|\mathfrak{A} - D_\xi A(x, \nabla u)\|_{L^\infty}$ is sufficiently small (and m sufficiently large), this implies the desired inf-sup-condition. In a similar fashion, one can also show that the bilinear form $(D_\xi A(x, \nabla u) \nabla \cdot, \nabla \cdot)$ satisfies an inf-sup-condition over $V_H \times V_H^{\text{ms}}$ if $\|\mathfrak{A} - D_\xi A(x, \nabla u)\|_{L^\infty}$ is sufficiently small. As a consequence, we can deduce with [37] that the solution $u_{H,m}^{PG}$ to (3.9) is well-defined and quasi-optimal for sufficiently small H . What is even more important is that we have the following quasi-optimality result in the L^2 -norm for the Petrov-Galerkin method (up to linearization errors), which corresponds well to the estimate in Corollary 4.3.

Theorem 4.5. *Let u be the solution to (2.2) and $u_{H,m}^{PG}$ the solution to (3.9). Let Assumptions 2.1 and 3.1 be satisfied. Furthermore, assume that $D_\xi A(x, \cdot)$ is Lipschitz continuous (in its second argument) in a neighborhood of ∇u and that there is $\gamma > 0$ independent of H and m such that*

$$\inf_{v_H \in V_H} \sup_{\psi_{H,m} \in V_{H,m}} \frac{|(D_\xi A(x, \nabla u) \nabla v_H, \nabla \psi_{H,m})|}{|v_H|_1 |\psi_{H,m}|_1} \geq \gamma. \quad (4.4)$$

Then it holds that

$$\begin{aligned}
|u - u_{H,m}^{PG}|_1 &\lesssim \inf_{v_H \in V_H} |u - v_H|_1, \\
\text{and } \|u - u_{H,m}^{PG}\|_0 &\lesssim \|u - I_H u\|_0 + (\|\mathfrak{A} - D_\xi A(x, \nabla u)\|_{L^\infty} + C_{\text{ol},m}^{1/2} \beta^m) \inf_{v_H \in V_H} |u - v_H|_1 \\
&\quad + \|R(u, u_{H,m}^{PG})\|_{H^{-1}(\Omega)}
\end{aligned}$$

with

$$\langle R(u, v), \psi \rangle := \int_{\Omega} \int_0^1 (D_{\xi} A(x, \nabla u + \tau \nabla(v - u)) - D_{\xi} A(x, \nabla u)) \nabla(v - u) \cdot \nabla \psi \, d\tau \, dx. \quad (4.5)$$

As already discussed after Corollary 4.3, the term $\|u - I_H u\|_0$ can essentially be replaced by the L^2 -best approximation error in V_H . This implies at least linear convergence and can yield up to quadratic convergence for sufficiently regular exact solutions for the choice $m \approx |\log H|$ and up to linearization errors, which are discussed in Section 4.3.

Proof of Theorem 4.5. The H^1 -semi norm estimate follows from the abstract theory in [37].

For the L^2 -estimate, we define $\tilde{u}_{H,m}^{PG} \in V_H$ as the unique solution to

$$(D_{\xi} A(x, \nabla u) \nabla \tilde{u}_{H,m}^{PG}, \nabla v_{H,m}) = (D_{\xi} A(x, \nabla u) \nabla u, \nabla v_{H,m}) \quad \text{for all } v_{H,m} \in V_{H,m}, \quad (4.6)$$

which is well-defined due to the inf-sup-condition (4.4). We split the error $u - u_{H,m}^{PG}$ into $u - \tilde{u}_{H,m}^{PG}$ and $\tilde{u}_{H,m}^{PG} - u_{H,m}^{PG}$ and estimate both parts separately.

Estimate of $\tilde{u}_{H,m}^{PG} - u_{H,m}^{PG}$: By Taylor expansion we obtain for any $v_{H,m} \in V_{H,m}$ that

$$\begin{aligned} & (A(x, \nabla u_{H,m}^{PG}), \nabla v_{H,m}) \\ &= (A(x, \nabla u), \nabla v_{H,m}) + (D_{\xi} A(x, \nabla u) \nabla (u_{H,m}^{PG} - u), \nabla v_{H,m}) + \langle R(u, u_{H,m}^{PG}), v_{H,m} \rangle. \end{aligned}$$

Thanks to Galerkin orthogonality, this implies

$$(D_{\xi} A(x, \nabla u) \nabla (u_{H,m}^{PG} - u), \nabla v_{H,m}) = -\langle R(u, u_{H,m}^{PG}), v_{H,m} \rangle. \quad (4.7)$$

Because of the inf-sup-condition (4.4), there exists $v_{H,m} \in V_{H,m}$ with $|v_{H,m}|_1 = 1$ such that

$$\begin{aligned} \|\tilde{u}_{H,m}^{PG} - u_{H,m}^{PG}\|_0 &\lesssim |\tilde{u}_{H,m}^{PG} - u_{H,m}^{PG}|_1 \lesssim (D_{\xi} A(x, \nabla u) \nabla (\tilde{u}_{H,m}^{PG} - u_{H,m}^{PG}), \nabla v_{H,m}) \\ &= (D_{\xi} A(x, \nabla u) \nabla (u - u_{H,m}^{PG}), \nabla v_{H,m}) = \langle R(u, u_{H,m}^{PG}), v_{H,m} \rangle \\ &\leq \|R(u, u_{H,m}^{PG})\|_{H^{-1}(\Omega)}, \end{aligned}$$

where we used Friedrich's inequality, (4.6), and (4.7).

Estimate of $u - \tilde{u}_{H,m}^{PG}$: This is in principle an L^2 -estimate for a Petrov-Galerkin LOD for a linear elliptic problem. However, the multiscale test space $V_{H,m}$ is built using \mathfrak{A} instead of $D_{\xi} A(x, \nabla u)$, which introduces additional error terms. First, we note that

$$|u - \tilde{u}_{H,m}^{PG}|_1 \lesssim \inf_{v_H \in V_H} |u - v_H|_1$$

because of the projection and the inf-sup-condition (4.4). Let $e_H := I_H u - \tilde{u}_{H,m}^{PG}$ and define $z_H^{\text{ms}} \in V_H^{\text{ms}}$ as the solution of the dual problem

$$(D_{\xi} A(x, \nabla u) \nabla \psi_H, \nabla z_H^{\text{ms}}) = (\psi_H, e_H)_{L^2(\Omega)} \quad \text{for all } \psi_H \in V_H.$$

This dual problem is well-posed because of the inf-sup-condition over $V_H \times V_H^{\text{ms}}$ as discussed after Lemma 4.4. We now obtain with the orthogonality of W and V_H^{ms} (w.r.t. \mathcal{A}) and Galerkin orthogonality that

$$\begin{aligned} \|e_H\|_0^2 &= (D_{\xi} A(x, \nabla u) \nabla e_H, \nabla z_H^{\text{ms}}) \\ &= (D_{\xi} A(x, \nabla u) \nabla (u - \tilde{u}_{H,m}^{PG}), \nabla z_H^{\text{ms}}) + ((\mathfrak{A} - D_{\xi} A(x, \nabla u)) \nabla (u - I_H u), \nabla z_H^{\text{ms}}) \\ &= (D_{\xi} A(x, \nabla u) \nabla (u - \tilde{u}_{H,m}^{PG}), \nabla (z_H^{\text{ms}} - z_{H,m})) + ((\mathfrak{A} - D_{\xi} A(x, \nabla u)) \nabla (u - I_H u), \nabla z_H^{\text{ms}}) \end{aligned}$$

for any $z_{H,m} \in V_{H,m}$. We write $z_H^{\text{ms}} = (\text{id} - \mathcal{Q})I_H z_H^{\text{ms}}$ and choose $z_{H,m} = (\text{id} - \mathcal{Q}_m)I_H z_H^{\text{ms}}$. Then we deduce with Proposition 4.1 and $|z_H^{\text{ms}}|_1 \lesssim \|e_H\|_0$ that

$$\|e_H\|_0^2 \lesssim C_{\text{ol},m}^{1/2} \beta^m |u - \tilde{u}_{H,m}^{PG}|_1 \|e_H\|_0 + \|\mathfrak{A} - D_\xi(x, \nabla u)\|_{L^\infty} |u - I_H u|_1 \|e_H\|_0.$$

The triangle inequality and the quasi-optimality of $\tilde{u}_{H,m}^{PG}$ finally yields

$$\|u - \tilde{u}_{H,m}^{PG}\|_0 \lesssim \|u - I_H u\|_0 + (C_{\text{ol},m}^{1/2} \beta^m + \|\mathfrak{A} - D_\xi A(x, \nabla u)\|_{L^\infty}) \inf_{v_H \in V_H} |u - v_H|_1,$$

which in combination with the estimate for $\tilde{u}_{H,m}^{PG} - u_{H,m}^{PG}$ finishes the proof. \square

4.3. Linearization errors

The linearization of the corrector computation has introduced several terms in our error estimates, which we all classify as linearization errors although they are of different nature. First and foremost, we have $\eta_{\text{lin}}(u)$ from Theorem 4.2. Second, there is the remainder of the Taylor expansion $R(u, v)$ in Theorem 4.5 and last, we have the error $\|\mathfrak{A} - D_\xi A(x, \nabla u)\|_{L^\infty}$. We first note that the boundedness of A and the stabilities of \mathcal{Q} and I_H directly imply that $\eta_{\text{lin}}(u) \lesssim |u|_1 \lesssim \|f\|_0$, i.e., this linearization error is bounded from above by a constant without any further assumptions. For a further analysis of the various linearization errors we make the following additional assumption on A .

Assumption 4.6. *We assume that $D_\xi A$ is Lipschitz continuous in its last argument, i.e., there is $L_A > 0$ such that*

$$|D_\xi A(x, \xi_1) - D_\xi A(x, \xi_2)| \leq L_A |\xi_1 - \xi_2| \quad \text{for all } \xi_1, \xi_2 \in \mathbb{R}^d \text{ and almost all } x \in \Omega.$$

Lemma 4.7. *Let Assumptions 2.1, 3.1, and 4.6 be satisfied and assume that all involved functions are sufficiently regular. Then we have the following estimates for the linearization errors*

$$\begin{aligned} \eta_{\text{lin}}(u) &\leq L_A \|\nabla(\text{id} - \mathcal{Q})I_H u\|_{L^\infty} |(\text{id} - \mathcal{Q})I_H u|_1, \\ \|R(u, v)\|_{H^{-1}(\Omega)} &\leq L_A \|\nabla(u - v)\|_{L^\infty} |u - v|_1 \\ \|\mathfrak{A} - D_\xi A(x, \nabla u)\|_{L^\infty} &\leq L_A \|\nabla u\|_{L^\infty}. \end{aligned}$$

Proof. The second and third estimate are obvious under Assumption 4.6. To estimate the $\eta_{\text{lin}}(u)$ we perform a Taylor expansion around zero and obtain due to (3.3) that for any $w \in W$ it holds that

$$(A(x, \nabla(\text{id} - \mathcal{Q})I_H u), \nabla w) = \int_\Omega \int_0^1 (D_\xi A(x, \tau \nabla((\text{id} - \mathcal{Q})I_H u)) - \mathfrak{A}) \nabla((\text{id} - \mathcal{Q})I_H u) \cdot \nabla w \, d\tau \, dx.$$

Again, Assumption 4.6 finishes the proof. \square

Only for the first and second linearization error we can hope to extract powers of H . Concerning the first estimate, we note that $|(\text{id} - \mathcal{Q})I_H u|_1$ is bounded (independent of H), so that one has to estimate the projection into the kernel space W in L^∞ . However, the maximum norm error estimates available for standard finite element space, see [8, Chapter 8], are not transferable. For the second estimate, we have $v = u_{H,m}^{PG} \in V_H$ for Theorem 4.5. Hence, $|u - u_{H,m}^{PG}|_1$ is bounded by the H^1 -best approximation in V_H . The results of [8, Chapter 8] might be applicable to extract a power of H in the L^∞ -term of the second estimate in this case. Yet, since we do not have a standard finite element method, this application needs to be carefully checked which is beyond the scope of the paper. Certainly, all estimates in Lemma 4.7 require higher regularity of the exact solution, which however is not available for the general case with spatial discontinuities of A . Thus the linearization errors remain a subject for future research.

5. Numerical experiments

We present the results of several numerical experiments, subject to different multiscale coefficients and non-linearities. In all cases, the computational domain is $\Omega = [0, 1]^2$. We use the Petrov-Galerkin method (3.9) and obtain a solution $u_{H,m}^{PG} \in V_H$, which is compared with a finite element reference solution $u_h \in V_h$ on the fine mesh. If fine-scale information of the coarse-scale solution is required, we compute $u_{H,m}^{LOD,PG} = (\text{id} - \mathcal{Q}_m)u_{H,m}^{PG}$ in a post-processing step as described in Section 3.2. We focus on two (relative) errors in the following: The so-called *(relative) upscaled error*

$$e_{\text{LOD}} := \frac{|u_h - u_{H,m}^{\text{LOD,PG}}|_1}{|u_h|_1}$$

between the reference and the upscaled solution in the H^1 -semi norm, for which we expect a linear convergence rate (cf. Theorem 4.2 for the Galerkin method); and the so-called *(relative) macroscopic error*

$$e_H := \frac{\|u_h - u_{H,m}^{PG}\|_0}{\|u_h\|_0}$$

between the reference and the Petrov-Galerkin solution (lying in the finite element space) in the L^2 -norm, for which we expect the same behavior as the L^2 -best approximation in V_H (cf. Theorem 4.5).

The reference mesh size is fixed as $h = 2^{-9}$ in all experiments and the coarse mesh size varies as $H = 2^{-2}, 2^{-3}, \dots, 2^{-7}$. We present results for oversampling parameters $m = 1, 2, 3$ and already point out that $m = 2, 3$ is a sufficient choice in most experiments. To solve the non-linear problems, we use the Newton method with zero start vector and tolerance 10^{-11} for the residual as stopping criterion. The non-linearity A in the first two examples is of the type specified in Assumption 2.1, whereas the other two examples consider a model for the stationary Richards equation with so-called quasi-linear coefficients of the form $A_2(x, u)\nabla u$. Note that the resulting non-linear form \mathcal{B} is no longer monotone such that the above proof techniques do not directly transfer, see [5, 6]. Nevertheless, we use the presented multiscale method with the obvious modifications for (3.9) and $\mathfrak{A} := A_2(x, 0)$ in the corrector problems.

5.1. Periodic coefficient

We choose a model problem similar to [2]. The non-linear coefficient is defined as

$$A(x, \xi) = \left(1 + x_1 x_2 + \frac{1.1 + \frac{\pi}{3} + \sin(2\pi \frac{x}{\varepsilon})}{1.1 + \sin(2\pi \frac{x}{\varepsilon})}\right) \left(1 + \frac{1}{(1 + |\xi|^2)^{1/2}}\right) \xi$$

with $\varepsilon = 2^{-5}$ and source $f(x) = 10 \exp(-0.1|x - x_0|^2)$ with $x_0 = (0.45, 0.5)^T$ in our case. The coefficient and the reference solution u_h are depicted in Figure 5.1. Note that one can hope for higher regularity of the exact solution u in this case.

The (relative) macroscopic errors e_H are depicted in Figure 5.2 (left). We note that the errors for $m = 2, 3$ closely follow the error of the (relative) L^2 -best approximation in the space V_H (cf. the discussion after Theorem 4.5). Since the solution $u_{H,m}^{PG}$ lies in the same space, we cannot hope for anything better. In particular, the reduced convergence rate for H between $\sqrt{\varepsilon}$ and ε is no defect of the method, but intrinsic to the problem, see also the discussion of this so-called resonance effect in [17]. We emphasize that in the pre-asymptotic range $H \ll \varepsilon$, the standard finite element method does not produce faithful results and also shows no convergence rates, while the presented multiscale method follows the best approximation error and converges with linear rate. Figure 5.2 (right) presents the results for the (relative) upscaled error e_{LOD} : For

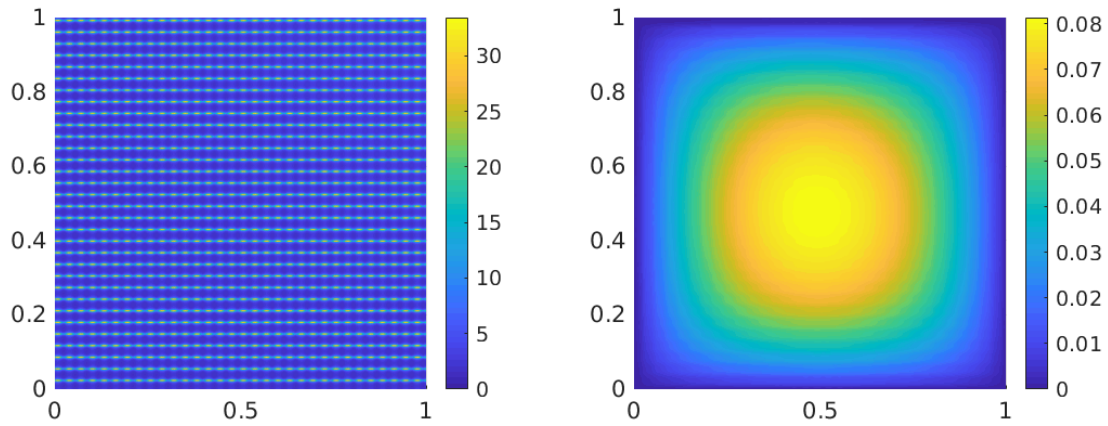


Figure 5.1: Spatial part of the coefficient (left) and reference solution u_h (right) for the experiment of Section 5.1.

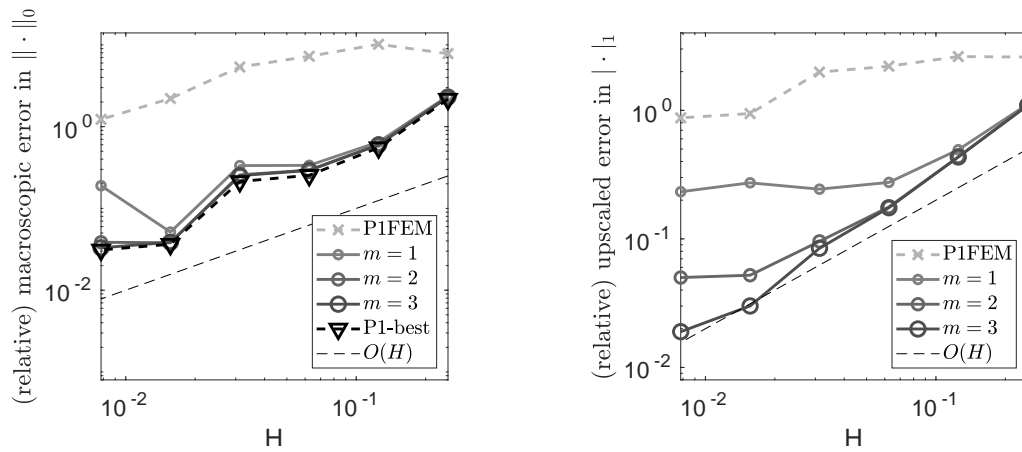


Figure 5.2: Convergence histories for the (relative) macroscopic error e_H (in L^2 -norm) (left) and the (relative) upscaled error e_{LOD} (in H^1 -semi norm) (left) for the experiment of Section 5.1.

approximations in the H^1 -semi norm, the (coarse-scale) space V_H is no longer sufficient, as also underlined by homogenization theory, but fine-scale features have to be taken in account. The error for the upscaled Petrov-Galerkin solution $u_{H,m}^{\text{LOD},PG}$ converges linearly, which is predicted for the Galerkin solution $u_{H,m}$ in Theorem 4.2. As emphasized earlier, $u_{H,m}^{\text{LOD},PG}$ and $u_{H,m}$ do not agree but presumably are very close. In fact, computations with the Galerkin method have shown (qualitatively and quantitatively) similar results. Since the Petrov-Galerkin method is favorable from the computational efficiency point of view, we hence solely focus on this variant and only upscale the coarse-scale solution as described if necessary. All in all, the experiment clearly confirms the predicted convergence rates of Theorems 4.2 and 4.5.

5.2. Random coefficient with possible high contrast

We choose the non-linear coefficient as

$$A(x, \xi) = c(x) \begin{pmatrix} \xi_1 + \frac{1}{3}\xi_1^3 \\ \xi_2 + \frac{1}{3}\xi_2^3 \end{pmatrix},$$

where $c(x)$ is piece-wise constant on a quadrilateral mesh \mathcal{T}_ε with $\varepsilon = 2^{-6}$ and the values are random numbers in $[0.1, 0.1\eta]$. We consider $\eta \in \{10, 100\}$ to highlight the influence of a growing contrast. In both cases, the right-hand side is

$$f(x) = \begin{cases} 0.1 & x_2 \leq 0.1, \\ 1 & \text{else,} \end{cases}$$

see [20] for the non-linearity and the right-hand side. Note that we clearly cannot expect higher regularity than $H_0^1(\Omega)$ for the exact solution in this case because of the spatial discontinuities in A . The coefficients and corresponding reference solutions u_h are depicted in Figure 5.3.

The convergence histories for the (relative) macroscopic error e_H are depicted in Figure 5.4. The standard FEM needs a mesh with $H \leq \varepsilon$ to obtain convergence because only then the coefficient A and in particular its jumps are resolved. The multiscale method, however, again follows the best approximation error even in the pre-asymptotic regime. Comparing the two choices of η , we observe a qualitatively similar behavior of all errors, but the relative errors for the higher contrast are at a higher level. However, one should also note the smaller values of the reference solution u_h (see Figure 5.3, bottom right) in this context.

As in the previous example, we also consider the error of the (relative) upscaled error e_{LOD} in Figure 5.5. We observe a saturation of the error for decreasing mesh width, but only for the low-contrast case, see Figure 5.5 left. Since the reference solution is smaller (values closer to zero) in total for the higher contrast, the linearization around zero might have less influence here so that we observe better convergence. Although not shown here, we note that the same effect occurs (qualitatively) also for the Galerkin variant, so that it is not caused by the difference between $u_{H,m}$ and $u_{H,m}^{\text{LOD},PG}$. Interestingly, the saturation effect for low contrast, however, does not show up in the macroscopic error e_H , which lies in the finite element space and uses the correctors in the test functions. So we may conclude that the linear correction computation is still good enough to improve the test functions in comparison to the standard finite element functions, but not sufficient to extract fine-scale information. Furthermore, Figure 5.5 shows that for higher contrast larger oversampling parameters are needed for optimal convergence, an observation which has been intensively studied in the linear case [18, 35].

This example confirms and underlines that the present multiscale method does not rely on assumptions such as periodicity or scale separation and thus also works in situations where no homogenization results are available.

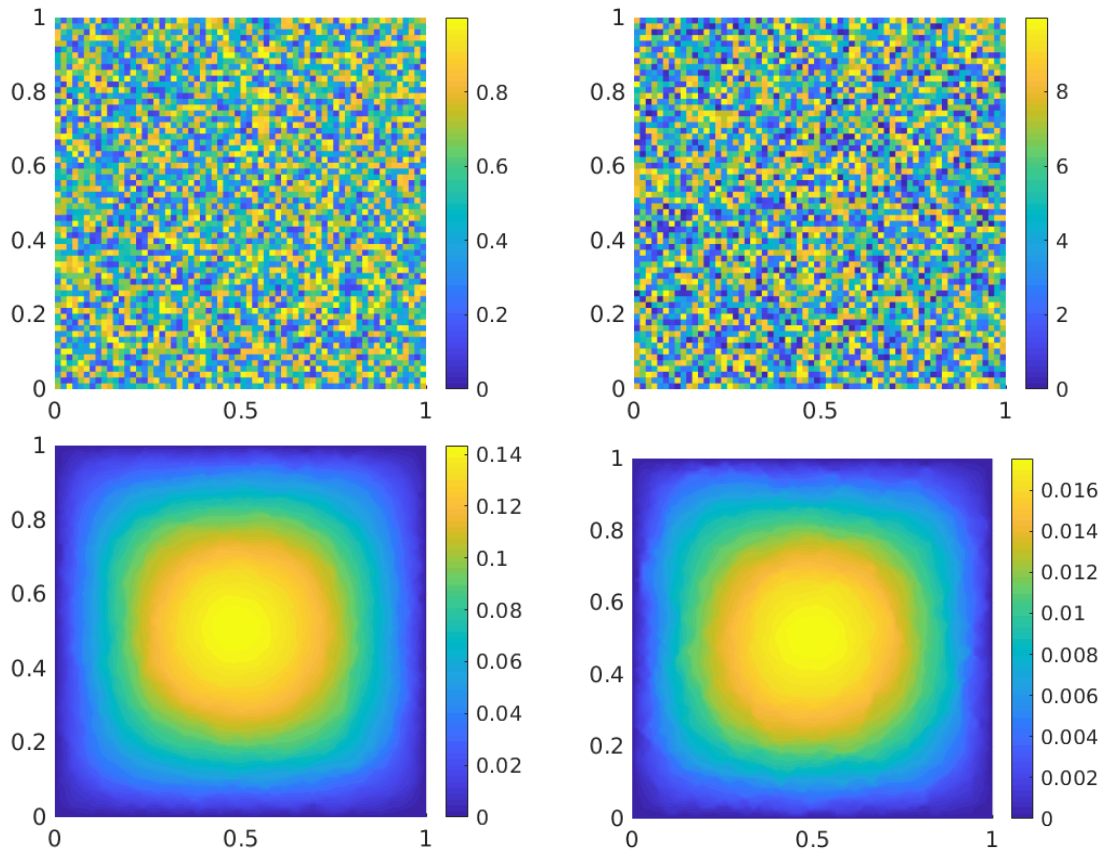


Figure 5.3: Spatial part of the coefficient (top) and reference solution u_h (bottom) with contrast $\eta = 10$ (left) and $\eta = 100$ (right) for the experiment of Section 5.2.

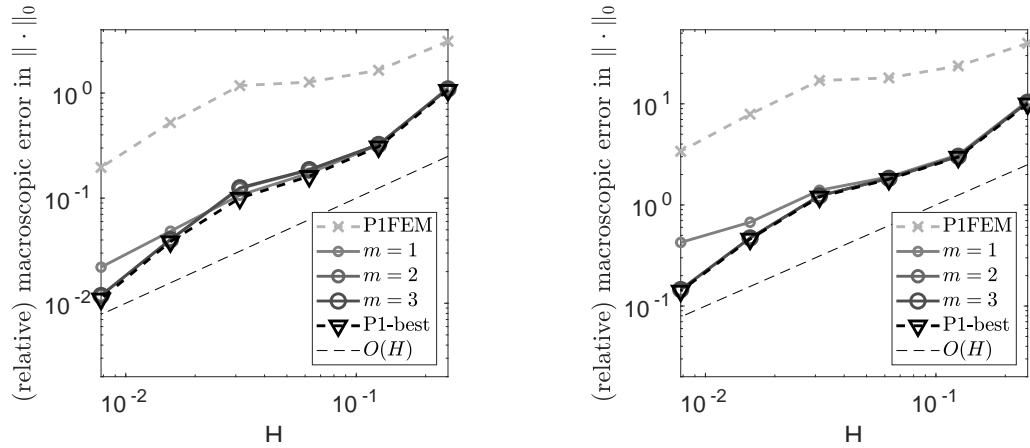


Figure 5.4: Convergence histories for the (relative) macroscopic error e_H (in L^2 -norm) with $\eta = 10$ (left) and $\eta = 100$ (right) for the experiment of Section 5.2.

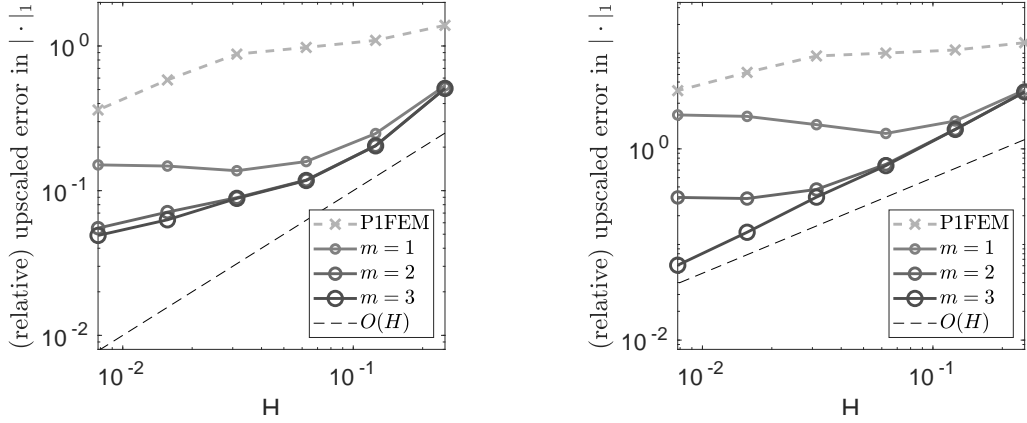


Figure 5.5: Convergence histories for the (relative) upscaled error e_{LOD} (in H^1 -semi norm) with $\eta = 10$ (left) and $\eta = 100$ (right) for the experiment of Section 5.2.

5.3. Stationary Richards equation – example 1

We now test the applicability of our method to quasi-linear non-monotone problems, which, for instance, are frequently encountered in (unsaturated) groundwater flow and can be modeled by the (stationary) Richards equation. The coefficient is of the form $A(x, s, \xi) = k(x, s)\xi$, where in this first example we choose for k a function as suggested in [1], namely

$$k(x, s) = 200\alpha_\varepsilon(x)e^{-\alpha_\varepsilon(x)(s-2)^2} + (x_1 - 0.3)^2 + x_2^2 + 2 \quad \text{with} \quad \alpha_\varepsilon(x) = \frac{0.0005}{2 + 1.8 \sin(2\pi \frac{x_1}{\varepsilon} - 6\pi \frac{x_2}{\varepsilon})}.$$

In the numerical experiment, we fix $\varepsilon = 2^{-5}$ and $f = 1$.

As in the non-linear case, we plot the errors e_{LOD} and e_H in Figure 5.6. The rates are even better than predicted by the theory for the Galerkin method for the non-linear monotone case. This is related to the high regularity of the right-hand side f , where higher convergence rates for the ideal method are known for $f \in H^1(\Omega)$ in the linear case, see [31]. This example shows that the method exploits possible higher regularity and more importantly, that it is not restricted to the monotone elliptic case, but also a dependence on u in the non-linearity can be incorporated. This illustrates that the method might be useful in a large range of practically interesting applications, even beyond the framework of the present numerical analysis.

5.4. Stationary Richards equation – example 2

This example continues the application to groundwater flow and geophysics with probably more realistic models. Here, we consider a quasi-linear coefficient of the form $A(x, s, \xi) = c(x)k(s)\xi$. For c we choose a spatial multiscale model with a channel as depicted in Figure 5.7 left, which is often present in geophysical applications. Note that this can easily be extended to the case of several channels. For the non-linearity k , we consider the following so-called van Genuchten model [39]

$$k(s) = \frac{(1 - \alpha|s|(1 + (\alpha|s|)^2)^{-1/2})^2}{1 + (\alpha|s|)^2}$$

with $\alpha = 0.005$, see also [11]. The right-hand side f is the same as described in Section 5.2. The reference solution for the present setting is depicted in Figure 5.7 right. Note the influence of

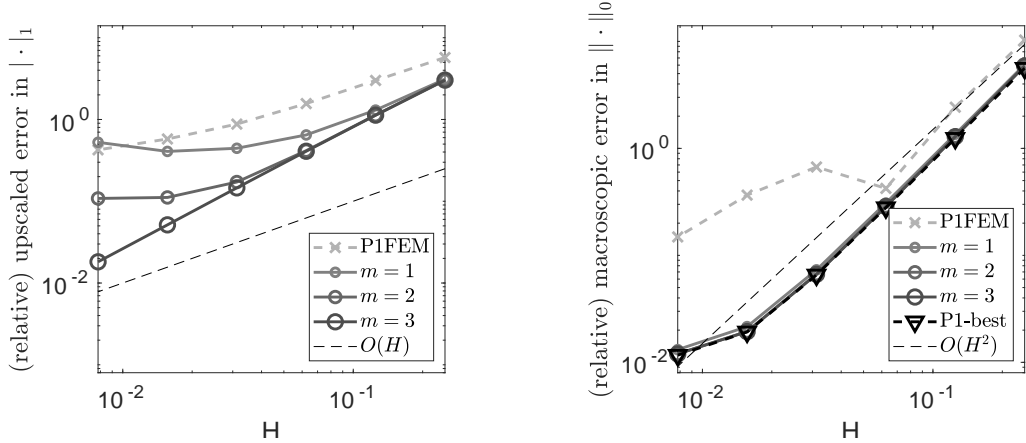


Figure 5.6: Convergence histories for the (relative) upscaled error e_{LOD} (in H^1 -semi norm) (left) and the (relative) macroscopic error e_H (in L^2 -norm) (right) for the experiment of Section 5.3.

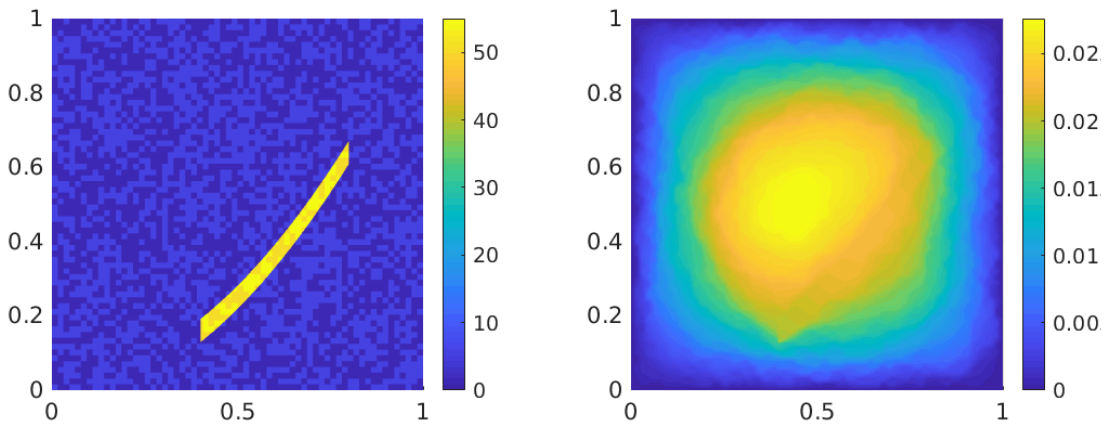


Figure 5.7: Coefficient $c(x)$ (left) and reference solution (right) for the experiment of Section 5.4.

the channel, which analytically manifests itself in a low regularity of the solution (in comparison with the experiment in Section 5.3, for instance).

As a consequence, we observe exactly the (worst-case) convergence rates as predicted by our theory (again for the non-linear monotone case only), but not more. In particular, the L^2 -error for the Petrov-Galerkin solution (which is in the finite element space) follows the best-approximation error, which in this case is “only” linear as discussed after Theorem 4.5. Furthermore, we (again) see a saturation or stagnation of the upscaled error e_{LOD} for decreasing mesh sizes as in the experiment of Section 5.2 with low-contrast. Here, it might be caused by the high-contrast channel (a different type of high contrast than in the random coefficient), which can be cured by a large choice of m or by more advanced interpolation operators, see [18, 35]. Another reason could be the rather steep gradient of the reference solution in vicinity of the channel (and thereby also a low regularity of the solution), which again may lead to rather large linearization errors. We hence see some possible limitations of the current method. However, these limits may be overcome by more sophisticated upscaling techniques or even a re-computation of the multiscale

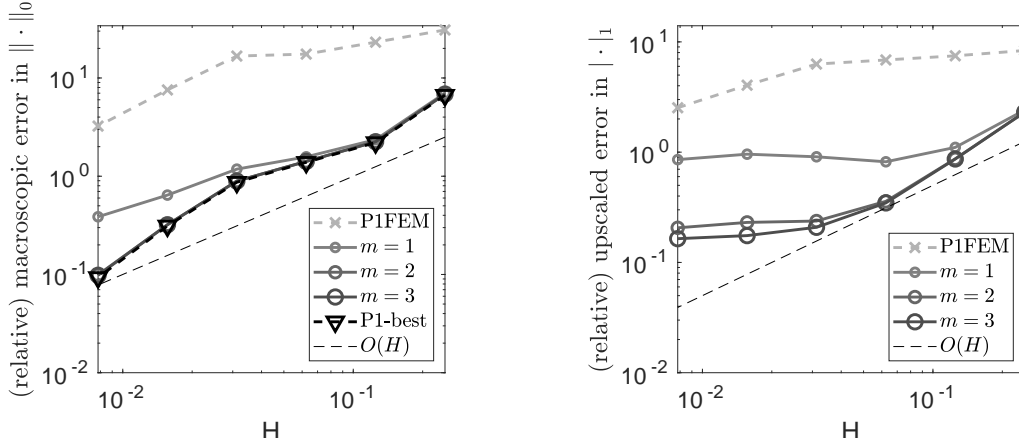


Figure 5.8: Convergence histories for the (relative) macroscopic error (in L^2 -norm) (left) and for the (relative) upscaled error e_{LOD} (in H^1 -semi norm) (right) for the experiment of Section 5.4.

basis at some steps in the Newton method. The latter requires some sort of error indicator, where [19] may serve as an inspiration, especially with view on the error caused by using \mathfrak{A} instead of $D_\xi A(x, \nabla u)$. Yet, we strongly emphasize that the (macroscopic) Petrov-Galerkin solution still is optimal as it almost coincides with the best approximation error, see Figure 5.8 left, which is a very promising result. This discrepancy between the good performance of the multiscale basis for the computation of the macroscopic part versus its failure for the upscaling needs to be investigated in future research.

Conclusion

We presented a multiscale method for non-linear monotone elliptic problems with spatial multi-scale features. A problem-adapted multiscale basis is constructed by solving local linear fine-scale problems for each coarse-scale mesh element. The new basis is employed in a generalized finite element method in either a Galerkin or a Petrov-Galerkin variant. Numerical analysis shows optimal error estimates up to linearization errors. Several numerical experiments underline and confirm the applicability of the method as well as the expected convergence rates. As mentioned, some questions remain open from the numerical analysis, in particular the good estimates for the linearization errors. Moreover, different upscaling techniques and/or linearization strategies for the corrector problems could be considered and compared. With respect to the promising numerical examples for quasi-linear non-monotone problems, the numerical analysis for this case is an interesting next project. A generalization of the method to other non-linear problems seems possible, here we note as interesting applications (besides Richards equation) porous media flow, non-linear elasticity, and wave propagation in non-linear media (e.g., of Kerr-type).

References

- [1] A. Abdulle, Y. Bai, and G. Vilmart. Reduced basis finite element heterogeneous multiscale method for quasilinear elliptic homogenization problems. *Discrete Contin. Dyn. Syst. Ser. S*, 8(1):91–118, 2015.

- [2] A. Abdulle and M. E. Huber. Error estimates for finite element approximations of nonlinear monotone elliptic problems with application to numerical homogenization. *Numer. Methods Partial Differential Equations*, 32(3):955–969, 2016.
- [3] A. Abdulle and M. E. Huber. Finite element heterogeneous multiscale method for nonlinear monotone parabolic homogenization problems. *ESAIM Math. Model. Numer. Anal.*, 50(6):1659–1697, 2016.
- [4] A. Abdulle, M. E. Huber, and G. Vilmart. Linearized numerical homogenization method for nonlinear monotone parabolic multiscale problems. *Multiscale Model. Simul.*, 13(3):916–952, 2015.
- [5] A. Abdulle and G. Vilmart. A priori error estimates for finite element methods with numerical quadrature for nonmonotone nonlinear elliptic problems. *Numer. Math.*, 121(3):397–431, 2012.
- [6] A. Abdulle and G. Vilmart. Analysis of the finite element heterogeneous multiscale method for quasilinear elliptic homogenization problems. *Math. Comp.*, 83(286):513–536, 2014.
- [7] G. Allaire. Homogenization and two-scale convergence. *SIAM J. Math. Anal.*, 23(6):1482–1518, 1992.
- [8] S. C. Brenner and L. R. Scott. *The mathematical theory of finite element methods*, volume 15 of *Texts in Applied Mathematics*. Springer-Verlag, New York, 1994.
- [9] E. Chung, Y. Efendiev, K. Shi, and S. Ye. A multiscale model reduction method for nonlinear monotone elliptic equations in heterogeneous media. *Netw. Heterog. Media*, 12(4):619–642, 2017.
- [10] P. G. Ciarlet. *The finite element method for elliptic problems*, volume 40 of *Classics in Applied Mathematics*. Society for Industrial and Applied Mathematics (SIAM), Philadelphia, PA, 2002.
- [11] Y. Efendiev, J. Galvis, S. Ki Kang, and R. D. Lazarov. Robust multiscale iterative solvers for nonlinear flows in highly heterogeneous media. *Numer. Math. Theory Methods Appl.*, 5(3):359–383, 2012.
- [12] Y. Efendiev, J. Galvis, G. Li, and M. Presho. Generalized multiscale finite element methods. Nonlinear elliptic equations. *Commun. Comput. Phys.*, 15(3):733–755, 2014.
- [13] Y. Efendiev, T. Y. Hou, and V. Ginting. Multiscale finite element methods for nonlinear problems and their applications. *Commun. Math. Sci.*, 2(4):553–589, 2004.
- [14] D. Elfverson, V. Ginting, and P. Henning. On multiscale methods in Petrov-Galerkin formulation. *Numer. Math.*, 131(4):643–682, 2015.
- [15] C. Engwer, P. Henning, A. Målqvist, and D. Peterseim. Efficient implementation of the localized orthogonal decomposition method. *Comput. Methods Appl. Mech. Engrg.*, 350:123–153, 2019.
- [16] M. Feistauer and A. Ženíšek. Finite element solution of nonlinear elliptic problems. *Numer. Math.*, 50(4):451–475, 1987.
- [17] D. Gallistl and D. Peterseim. Computation of quasi-local effective diffusion tensors and connections to the mathematical theory of homogenization. *Multiscale Model. Simul.*, 15(4):1530–1552, 2017.

- [18] F. Hellman and A. Målqvist. Contrast independent localization of multiscale problems. *Multiscale Model. Simul.*, 15(4):1325–1355, 2017.
- [19] F. Hellman and A. Målqvist. Numerical homogenization of elliptic PDEs with similar coefficients. *Multiscale Model. Simul.*, 17(2):650–674, 2019.
- [20] P. Henning. *Heterogeneous multiscale finite element methods for advection-diffusion and nonlinear elliptic multiscale problems*. PhD thesis, WWU Münster, 2011.
- [21] P. Henning and A. Målqvist. Localized orthogonal decomposition techniques for boundary value problems. *SIAM J. Sci. Comput.*, 36(4):A1609–A1634, 2014.
- [22] P. Henning, A. Målqvist, and D. Peterseim. A localized orthogonal decomposition method for semi-linear elliptic problems. *ESAIM Math. Model. Numer. Anal.*, 48(5):1331–1349, 2014.
- [23] P. Henning, A. Målqvist, and D. Peterseim. Two-level discretization techniques for ground state computations of Bose-Einstein condensates. *SIAM J. Numer. Anal.*, 52(4):1525–1550, 2014.
- [24] P. Henning and M. Ohlberger. Error control and adaptivity for heterogeneous multiscale approximations of nonlinear monotone problems. *Discrete Contin. Dyn. Syst. Ser. S*, 8(1):119–150, 2015.
- [25] P. Henning and D. Peterseim. Oversampling for the multiscale finite element method. *Multiscale Model. Simul.*, 11(4):1149–1175, 2013.
- [26] V. H. Hoang. Sparse finite element method for periodic multiscale nonlinear monotone problems. *Multiscale Model. Simul.*, 7(3):1042–1072, 2008.
- [27] M. Huber. *Numerical homogenization methods for advection-diffusion and nonlinear monotone problems with multiple scales*. PhD thesis, EPFL, 2015.
- [28] R. Kornhuber, D. Peterseim, and H. Yserentant. An analysis of a class of variational multiscale methods based on subspace decomposition. *Math. Comp.*, 87(314):2765–2774, 2018.
- [29] R. Kornhuber and H. Yserentant. Numerical homogenization of elliptic multiscale problems by subspace decomposition. *Multiscale Model. Simul.*, 14(3):1017–1036, 2016.
- [30] D. Lukkassen, G. Nguetseng, and P. Wall. Two-scale convergence. *Int. J. Pure Appl. Math.*, 2(1):35–86, 2002.
- [31] A. Målqvist and D. Peterseim. Localization of elliptic multiscale problems. *Math. Comp.*, 83(290):2583–2603, 2014.
- [32] H. Owhadi. Multigrid with rough coefficients and multiresolution operator decomposition from hierarchical information games. *SIAM Rev.*, 59(1):99–149, 2017.
- [33] H. Owhadi and L. Zhang. Localized bases for finite-dimensional homogenization approximations with nonseparated scales and high contrast. *Multiscale Model. Simul.*, 9(4):1373–1398, 2011.

- [34] D. Peterseim. Variational multiscale stabilization and the exponential decay of fine-scale correctors. In *Building bridges: connections and challenges in modern approaches to numerical partial differential equations*, volume 114 of *Lect. Notes Comput. Sci. Eng.*, pages 341–367. Springer, Cham, 2016.
- [35] D. Peterseim and R. Scheichl. Robust numerical upscaling of elliptic multiscale problems at high contrast. *Comput. Methods Appl. Math.*, 16(4):579–603, 2016.
- [36] D. Peterseim, D. Varga, and B. Verfürth. From domain decomposition to homogenization theory. In *DD25 proceedings (to appear)*. Springer, 2019.
- [37] J. Pousin and J. Rappaz. Consistency, stability, a priori and a posteriori errors for Petrov-Galerkin methods applied to nonlinear problems. *Numer. Math.*, 69(2):213–231, 1994.
- [38] L. A. Richards. Capillary conduction of liquids through porous mediums. *Physics*, 1(5):318–333, 1931.
- [39] M. van Genuchten. A closed form equations for predicting the hydraulic conductivity of unsaturated soils. *Soil Sci. Soc. Am. J.*, 40:892–898, 1980.
- [40] E. Zeidler. *Nonlinear functional analysis and its applications. IV. Applications to mathematical physics*. Springer-Verlag, New York, 1988.

A. L^2 -error estimate for the Galerkin method

In this appendix, we prove an L^2 -estimate for the Galerkin method (3.5).

Theorem A.1. *Let Assumptions 3.1 and 2.1 be fulfilled. Let u be the solution to (2.2) and $u_{H,m}$ the solution to (3.8). Then it holds that*

$$\|u - u_{H,m}\|_0 \lesssim (H + C_{\text{ol},m}^{1/2} \beta^m + \|\mathfrak{A} - D_\xi A(x, \nabla u)\|_{L^\infty}) |u - u_{H,m}|_1 + \|R(u, \tilde{u}_{H,m})\|_{H^{-1}(\Omega)}$$

with the remainder R from (4.5) and where $\tilde{u}_{H,m}$ is defined via (A.1) below.

The first term of the above error estimate presumably is of $O(H^2)$ for the choice $m \approx |\log H|$ (up to the linearization error $\|\mathfrak{A} - D_\xi A(x, \nabla u)\|_{L^\infty}$). According to Lemma 4.7, we need to estimate $|u - \tilde{u}_{H,m}|_1$ and $\|\nabla(u - \tilde{u}_{H,m})\|_{L^\infty}$ for the remainder R in the second term. As shown below, $|u - \tilde{u}_{H,m}|_1$ is of order H (up to linearization terms). However, it is not clear whether $W^{1,\infty}$ -estimates for the multiscale space $V_{H,m}$ can be established in the spirit of [8, Chapter 8] to obtain a quadratic rate for the remainder R in total.

Proof. We use similar ideas as in the proof of Theorem 4.5. Let $\tilde{u}_{H,m} \in V_{H,m}$ be the unique solution to

$$(D_\xi A(x, \nabla u) \nabla \tilde{u}_{H,m}, \nabla v_{H,m}) = (D_\xi A(x, \nabla u) \nabla u, \nabla v_{H,m}) \quad \text{for all } v_{H,m} \in V_{H,m}, \quad (\text{A.1})$$

cf. [2]. We split the error $u - u_{H,m}$ into $u - \tilde{u}_{H,m}$ and $\tilde{u}_{H,m} - u_{H,m}$ and estimate both parts separately.

First step: Estimate of $\tilde{u}_{H,m} - u_{H,m}$: By Taylor expansion we obtain for any $v_{H,m} \in V_{H,m}$ that

$$\begin{aligned} & (A(x, \nabla \tilde{u}_{H,m}), \nabla v_{H,m}) \\ &= (A(x, \nabla u), \nabla v_{H,m}) + (D_\xi A(x, \nabla u) \nabla (\tilde{u}_{H,m} - u), \nabla v_{H,m}) + \langle R(u, \tilde{u}_{H,m}), v_{H,m} \rangle \\ &= (A(x, \nabla u_{H,m}), \nabla v_{H,m}) + \langle R(u, \tilde{u}_{H,m}), v_{H,m} \rangle, \end{aligned}$$

where we used Galerkin orthogonality and (A.1) in the last step. The estimate for $u_{H,m} - \tilde{u}_{H,m}$ now follows from Assumption 2.1 as

$$\begin{aligned} |u_{H,m} - \tilde{u}_{H,m}|_1^2 &\lesssim \left(A(x, \nabla u_{H,m}) - A(x, \nabla \tilde{u}_{H,m}), \nabla(u_{H,m} - \tilde{u}_{H,m}) \right) \\ &\leq \|R(u, \tilde{u}_{H,m})\|_{H^{-1}(\Omega)} |u_{H,m} - \tilde{u}_{H,m}|_1. \end{aligned}$$

The L^2 -estimate is obtained by applying Friedrich's inequality.

Second step: Estimate of $u - \tilde{u}_{H,m}$: This is in principle an L^2 -estimate for a Galerkin LOD for an elliptic diffusion problem. The main issue, however, is that the multiscale space $V_{H,m}$ is not built with respect to the diffusion tensor $D_\xi A(x, \nabla u)$ but with respect to $\mathfrak{A} = D_\xi A(x, 0)$. We first of all note that due to the projection, we have

$$|u - \tilde{u}_{H,m}|_1 \lesssim \inf_{v_{H,m} \in V_{H,m}} |u - v_{H,m}|_1 \leq |u - u_{H,m}|_1.$$

Let now $z \in H_0^1(\Omega)$ and $z_{H,m} \in V_{H,m}$ be the solutions of the following dual problems

$$\begin{aligned} (D_\xi A(x, \nabla u) \nabla v, \nabla z) &= (v, u - \tilde{u}_{H,m}) \quad \text{for all } v \in H_0^1(\Omega), \\ \text{and } (D_\xi A(x, \nabla u) \nabla v_{H,m}, \nabla z_{H,m}) &= (v_{H,m}, u - \tilde{u}_{H,m}) \quad \text{for all } v_{H,m} \in V_{H,m}. \end{aligned}$$

The ellipticity of $D_\xi A(x, \nabla u)$ and Galerkin orthogonality imply

$$\begin{aligned} |z - z_{H,m}|_1 &\lesssim \inf_{v_{H,m} \in V_{H,m}} |z - v_{H,m}|_1 \leq |z - (\text{id} - \mathcal{Q}_m)I_H z|_1 \\ &\leq |z - (\text{id} - \mathcal{Q})I_H z|_1 + |(\mathcal{Q} - \mathcal{Q}_m)I_H z|_1, \end{aligned}$$

where the last term can be estimated with Proposition 4.1. For the first term, we obtain with the ellipticity of \mathfrak{A} as well as the definitions of \mathcal{Q} and z that

$$\begin{aligned} |z - (\text{id} - \mathcal{Q})I_H z|_1^2 &\lesssim \mathcal{A}(z - (\text{id} - \mathcal{Q})I_H z, z - (\text{id} - \mathcal{Q})I_H z) \\ &= \mathcal{A}(z, z - (\text{id} - \mathcal{Q})I_H z) \\ &= ((\mathfrak{A} - D_\xi A(x, \nabla u)) \nabla z, \nabla(z - (\text{id} - \mathcal{Q})I_H z)) + (u - \tilde{u}_{H,m}, z - (\text{id} - \mathcal{Q})I_H z) \\ &\lesssim (\|\mathfrak{A} - D_\xi A(x, \nabla u)\|_{L^\infty} + H) \|u - \tilde{u}_{H,m}\|_0 |z - (\text{id} - \mathcal{Q})I_H z|_1. \end{aligned}$$

Combining the foregoing estimates, we conclude

$$|z - z_{H,m}|_1 \lesssim (H + C_{\text{ol},m}^{1/2} \beta^m + \|D_\xi A(x, 0) - D_\xi A(x, \nabla u)\|_{L^\infty}) \|u - \tilde{u}_{H,m}\|_0.$$

Finally, the definition of the dual problems yields

$$\begin{aligned} \|u - \tilde{u}_{H,m}\|_0^2 &= (D_\xi A(x, \nabla u) \nabla(u - \tilde{u}_{H,m}), \nabla z) \\ &= (D_\xi A(x, \nabla u) \nabla(u - \tilde{u}_{H,m}), \nabla(z - z_{H,m})) \\ &\lesssim |z - z_{H,m}|_1 \|u - \tilde{u}_{H,m}\|_1, \end{aligned}$$

which in combination with the already derived estimates finishes the proof. \square